Paper published on J. Micromech. Microeng. ***20*** *(2010) 045029 (9pp)*

Fabrication of MEMS components using ultra fine grained aluminium alloys

Xiao Guang Qiao[1, a], Nong Gao[1, b], Zakaria Moktadir[2, c], Michael Kraft[2, d] and Marco J Starink[1, e]
[1]Materials Research Group, School of Engineering Sciences,
[2]School of Electronics and Computer Science,
University of Southampton, Southampton SO17 1BJ, UK
Email: [a] xq@soton.ac.uk, [b] N.Gao@soton.ac.uk, [c] zm@ecs.soton.ac.uk
[d] mk1@ecs.soton.ac.uk [e] M.J.Starink@soton.ac.uk

Abstract. A novel process for the fabrication of a microelectromechanical systems (MEMS) metallic component with features smaller than 10 μm and high thermal conductivity was investigated. These may be applied in new or improved microscale components, such as (micro-) heat exchangers. In the first stage of processing, equal channel angular pressing (ECAP) was employed to refine the grain size of commercial purity aluminium (Al-1050) to the ultra fine grain (UFG) material. Embossing was conducted using a micro silicon mould fabricated by deep reactive ion etching (DRIE). Both cold embossing and hot embossing were performed on the coarse-grained and UFG Al-1050. Cold embossing on the UFG Al-1050 led to a partially transferred pattern from the micro silicon mould and high failure rate of the mould. Hot embossing on the UFG Al-1050 provided a smooth embossed surface with fully transferred pattern and low failure rate of the mould, while hot embossing on the coarse-grained Al-1050 resulted in a rougher surface with shear bands.

PACS: 85.85.+j

1. Introduction

If metals with a fine pattern of channels, typically below 10μm, can be reliably produced, then they may find application in a range of new or improved microdevices. One relevant device is a micro heat exchanger, which is a crucial component of many microelectromechanical systems (MEMS). Their efficiency is determined predominantly by size and density of cooling channels and the heat conductivity of the material from which it is fabricated. Fine, high density channels in a metal with high conductivity can strongly improve efficiency as compared to incumbent heat exchanger technology.

Micro heat exchangers were first investigated for very-large-scale integrated (VLSI) circuits [1] because the advent of systems employing high-speed, high-density VLSI circuits implies the requirement for effective and compact heat removal. Actually, micro heat exchangers can be applied in many important fields [2] where lightweight, small heat exchangers are required. One way to make a micro heat exchanger is to perform deep reactive ion etching (DRIE) on silicon wafers to get the micro heat exchanger components with micro scaled patterns [3]. An alternative method to produce micro heat exchangers uses the silicon chips with micro scale patterns by DRIE as a mould and transfers the patterns to a polymer by hot embossing [4]. This technique makes it easier to automatise production. However, polymers are generally not an ideal material for a micro heat exchanger because of low thermal conductivity. High thermal conductive metals with low costs such as aluminium and copper have been used extensively to fabricate traditional heat exchangers, and micro heat exchangers with channel size in a scale of hundreds of micrometers fabricated of steel, copper and titanium by diamond machining have been reported [5,6,7,8]. However, only very few studies on fabrication of metallic micro channels at micrometer scale using embossing method are reported. Otto et al. [9] attempted to fabricate optical components with micro channels in

size of a few micrometers by cold embossing using conventional coarse grained aluminium. The embossed surface showed uneven and rounded planks with ridges. Jiang et al [10] did a further attempt to emboss a coarse grained pure aluminium with a small area (2 mm × 2 mm) at ambient temperature using silicon mould with parallel channels with a width of 11.7 μm. A very high mould failure rate was observed due to misalignment of embossing. Böhm et al. [11] studied straight channels and complex structures fabricated by cold and superplastic embossing using a silicon die in various relatively fine materials (grain size > 3μm) including pure aluminium, stainless steel, pure copper and brass CuZn37. The minimum structure width was 10 μm. The cold embossed surface showed a better quality than their previous attempts [9], which is due to the finer grain, although the channel edges were still rounded. In order to achieve complete moulding of the structure a compressive stress much higher than the yield stress proved necessary. A significant lower loading force was observed during complex structure embossing of the Zn78Al22 alloys at elevated temperature, but the channel edges were still rounded which is due to superplastic deformation by grain boundary sliding and grain rotation[11]. The problems reported in the literature are thought to be related, amongst others, to the difficulty in reliably embossing metals with conventional microstructures.

In severe plastic deformation (SPD), conventional microstructures materials are changed to submicron or nano-scaled ones [12,13]. Equal channel angular pressing (ECAP) is one of the most effective processing method among the group of SPD methods [14], and it can be performed on a single specimen repeatedly because the specimen's cross section shape does not change during ECAP processing. Materials with submicron or nano-scaled grains produced by ECAP processing are low cost, low porosity, low oxide content and safe compared with the counterparts by gas condensation and mechanical alloying [12, 15]. Although extensive research has been carried out on the microstructure and property of ECAP processed alloys during the last decade [15, 16, 17], the application of ECAP processed materials and the exploitation of the ultra fine grain structure are still a subject of extensive research.

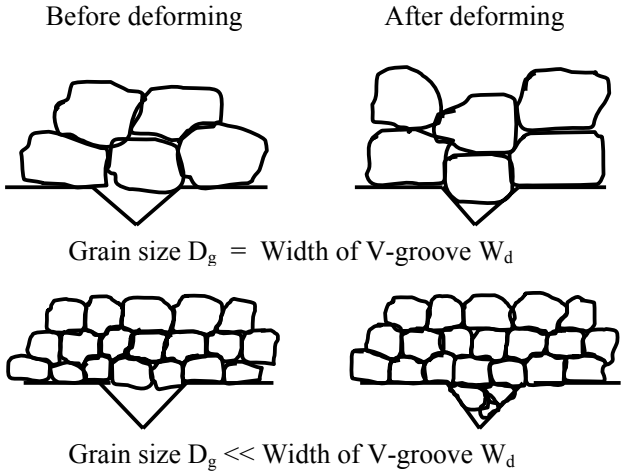

Figure 1 Schematic illustration of the difficulty associated with forming of features that are smaller than the grain size in polycrystalline materials. [19]

The current study is the first attempt to produce metallic foils with features at the scale of 5-50 μm by embossing using ultra-fine grained (UFG) aluminium alloys produced by equal channel angular pressing (ECAP). Performing embossing on aluminium alloys by silicon mould is rarely attempted because the aluminium alloys are much harder than polymers, which can cause failure of the silicon die [10]. Furthermore, conventional aluminium alloys have a grain size of > 50 μm, which is larger than the features we wish to produce by embossing, leading to large local deviations of forming force and channel size [18]. Figure 1 is a schematic illustration of this size effect [19]. During the fabrication of micro channels by

superplastic deformation of metals, the mould is filled by grain boundary sliding and grain rotation rather than intragranular deformation, which results in that micro components with sharp edges cannot be accurately formed by coarse grained metals. In an attempt to overcome this, we used UFG aluminium alloys with the grain size of ~ 1 μm to fabricate micro channels, which may be applied in the micro heat exchanger.

2. Theory

During ECAP, shear deformation occurs without change in billet cross section shape and severe plastic strain can accumulate by repeating the process for several passes. An equation for calculating the accumulated strain was initially provided by Segal et al [20] and further developed to a widely accepted and generally applicable equation by Iwahashi et al. [21]:

$$\varepsilon_N = \frac{N}{\sqrt{3}}\left[2\cot\left(\frac{\Phi}{2}+\frac{\Psi}{2}\right)+\Psi\cos\left(\frac{\Phi}{2}+\frac{\Psi}{2}\right)\right] \quad (1)$$

where ε_N is the accumulated shear strain value increment after N passes through the channels, Φ is the channel intersection angle and Ψ is the angle of curvature on the outer side of channel intersection (see Figure 2). Eq.(1) has been verified to be accurate by finite element modelling [22] and experiments [23] when frictional effects were ignored.

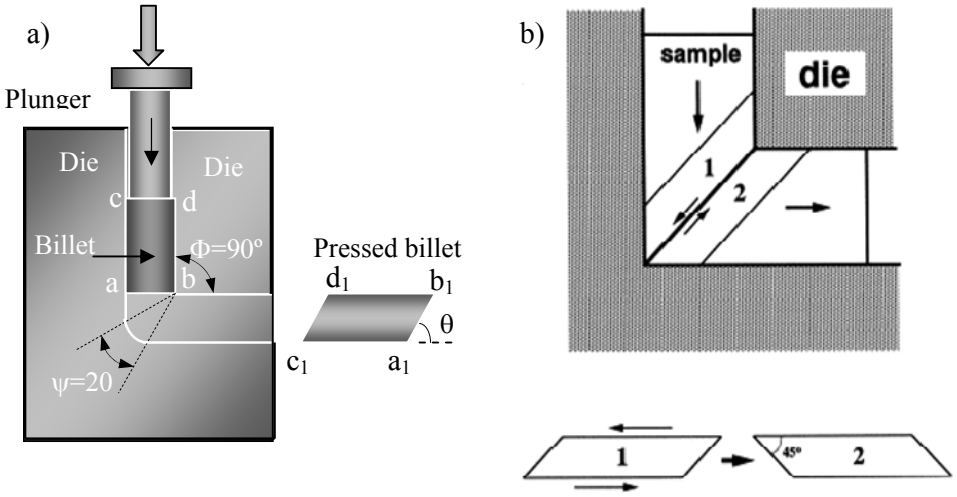

Figure2 Schematic diagrams showing a) the basic geometries ECAP die and billet pressed through it; and b) shear deformation in a billet, which is concentrated in the plane that is the intersection of the two die channels. [25]

The grain refinement during ECAP depends on total strain, route [24], temperature, alloy composition and backpressure. A recent quantitatively predictive model of grain refinement during SPD gives an accurate grain size including most of the above factors [13]. In this model, at the early stage of deformation during ECAP, a very high dislocation density is introduced, which leads to the formation of an intragranular structure consisting of cells with thick cell walls and low angles of misorientation. On increasing deformation dislocations are continuously generated, and accumulate at the cell wall/grain boundary. As a result, the thickness of the cell walls decreases, the misorientation between cell walls increases and the cell wall transfers to the grain boundary gradually. The basic calculation procedure of the model is given in Eq. (2) - Eq. (5). The increased strength $\Delta\sigma$ and dislocation density ρ during ECAP follows the classical equation given in Eq. (2), where α_1 is a constant, G is the shear modulus, b is the Burgers vector and M is Taylor factor. The increased strength $\Delta\sigma$ and plastic strain ε_p also obey a parabolic relationship with a proportion factor of K_A (see Eq. (3)). The value of K_A can be obtained by the tensile test or calculated by composition and

precipitates (see Ref [13]). The dislocation density in grains was ignored since it is much smaller than the dislocation density in the grain boundary, then the grain (in a Poisson-Voronoi shape) size d is related to the dislocation density by Eq.(4) and calculated by Eq.(5), where Sv is boundary area per unit volume, θ and $\bar{\theta}$ are misorientation and average misorientation angle between cells/grains, respectively, $\bar{L}$ is the mean lineal intercept length. In Eq. (5), the ρ_{GB} can be obtained by total strain when substituting Eq.(2) in Eq.(3) and assuming $\bar{\theta}$ constant ($\bar{\theta}$ is deduced from experimental measurements). We then have:

$$\Delta\sigma = M\tau = M\alpha_1 Gb\sqrt{\rho} \quad (2)$$

$$\Delta\sigma = G\alpha_1\sqrt{\frac{Mb}{l_d}}\sqrt{\varepsilon_p} = K_A \sqrt{\varepsilon_p} \quad (3)$$

$$\rho_{GB} = \int 1.5\frac{\theta}{b}\mathrm{d}S_{V,def} \cong 1.5\frac{\bar{\theta}}{b}S_V = 1.5\frac{\bar{\theta}}{b} * \frac{2}{\bar{L}} = 1.5\frac{\bar{\theta}}{b} * \frac{2.91}{d} \quad (4)$$

$$d \cong 2.91/S_{v,def} = 1.5 * 2.91\frac{\bar{\theta}}{\rho_{GB} b} \quad (5)$$

3. Materials and experimental Methods

3.1. Materials and characterizations

This study was carried out on Al-1050 aluminium, which is commercial purity aluminium with composition Al-0.18Fe-0.12Si (in wt. %) with further minor impurities. (Note that Fe and Si are the two most abundant impurities in aluminium, the price of Al increase strongly with increasing purity.) Al-1050 was supplied as an extruded rod of 4 m length and 9.53 mm diameter. Electron backscattered diffraction (EBSD) was used to characterize the microstructure as well as grain and subgrain boundary misorientation distribution in both as-received and UFG Al-1050. Samples of 10 mm length used for EBSD analysis were machined from the middle of ECAP-processed billets. For sample preparation, the surface of cross section was first mechanically ground up to 4000-grit SiC paper, then electropolished employing an electrolyte composed of 33 vol% nitric acid and 67 vol% methanol. The electropolishing was carried out with a DC voltage of 20-30 V for 30 seconds. The electrolyte was maintained at a temperature of -30˚C using liquid nitrogen. The equipment used was a JEOL JSM6500F thermal field emission gun scanning electron microscope (FEG-SEM) equipped with an HKL EBSD detector and HKL Channel 5 software. The SEM accelerating voltage was set to 15 kV. The step size was 4 μm for as-received Al-1050 and 0.1 μm for UFG Al-1050. Orientation imaging microscopy (OIM) maps were obtained from the cross section perpendicular to the longitudinal direction of ECAP-processed billets. Intercept lengths were determined using an automated procedure. For misorientation angle distributions the lowest cut off angle was set at 3˚.

The topography of micro silicon mould was observed by the JEOL JSM6500F FEG-SEM. The etching depth of the micro silicon mould was measured in second electron mode using the same FEG-SEM. The FEG-SEM and an Olympus BH-2 optical microscope (OM) equipped with a Prosilica digital CCD camera were used to observe the cross-section and embossed surface of the UFG aluminium foils. A Carl Zeiss XB1540 Focussed ion beam (FIB) was used to characterize the microstructure on the cross-section of the hot embossed foil. The FIB was operated at 30 kV with ion beam current of 200 pA.

To study recrystallization behaviour, ECAP-processed billets were annealed from 200 ˚C to 500 ˚C with a step size of 50 ˚C for 0.5 h at each temperature. The heat treated billets were machined to samples of 2 mm thickness for micro hardness testing. The circular surface was ground by abrasive papers from 600 grit to 1200 grit. Micro hardness testing was carried out on the circular surface. The hardness of each sample was calculated through averaging the measurements of five individual indentations on different locations close to the centre. Micro

hardness was tested on an MHT-1 model micro Vickers hardness tester. A force of 300 g was applied and holding time was 15 second.

3.2. Fabrication of UFG aluminium alloys

To produce an ultra fine grained (UFG) material ECAP was performed at room temperature. The lubricated metal billet of length 65 mm was pressed through a die containing two channels, equal in cross-section (9.7 mm diameter), intersecting at an angle Φ=90º (Figure 2 a)). During pressing, the billet undergoes severe shear deformation (Figure 2 b)) [25] but retains the same cross-sectional geometry so that it is possible to repeat the pressing operation for several consecutive passes through the die to impose very high accumulative strains. The equivalent strain after one pass of ECAP is about 100% (see Eq.(1)). The ECAP process was conducted up to 12 passes. (Further details on ECAP processing are provided in Ref [26].)

3.3. Fabrication of silicon mould

The micro silicon die was fabricated by the PEGASUS™ deep reactive ion etching (DRIE) machine from Surface Technology System plc. The UV-photo resist used for photolithography before DRIE was a S1818 model negative resist with a thickness of 2 μm from Shipley Corporation. The micro silicon die is a square plate with side length of 14 mm and thickness of 0.5 mm. The pattern on centre of the micro silicon die, which is 10 mm long and 10 mm wide, is a series of parallel straight channels, which are 10 μm deep and 10 μm wide with 10 μm grating.

The SEM image of the micro silicon die (Figure 3) shows that the channel bottom is smooth. However, scallops can be seen on the side wall of the channels due to the cyclic alternation between etch and passivation steps. The measured depth of the channel is on average 10.03 μm.

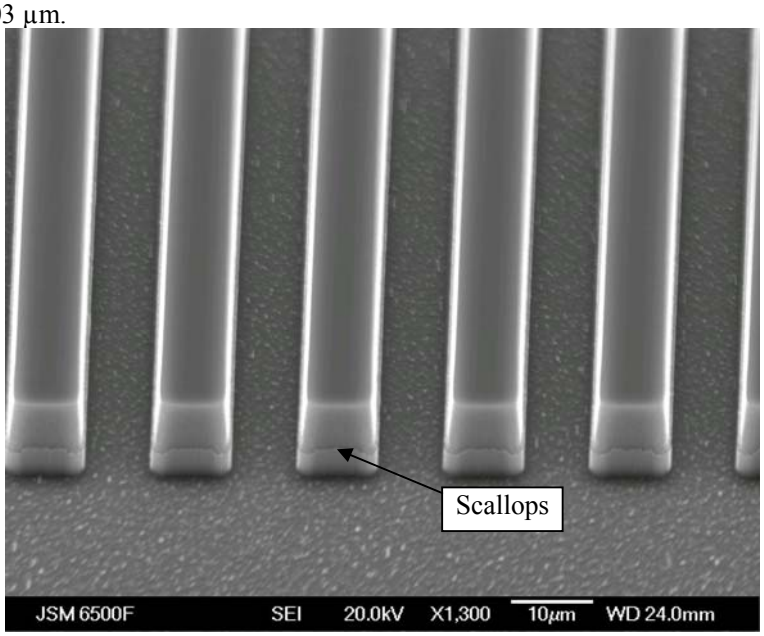

Figure3 SEM image of micro silicon die with the channel depth of 10 μm and width of 10 μm.

3.4. Cold embossing procedure and rigs set up

The embossing process was carried out at ambient temperature on a 9510 Instron testing machine with maximum capacity of 10 kN (see Figure 4). Platens and fixture were specially designed to fit the machine. Samples of 1 mm thickness were machined from ECAP-processed billets along the longitudinal direction for embossing. The circular surface was ground by abrasive papers from 600 grits to 1200 grits then polished to mirror-like surface. The embossing process was carried out on the circular surface by the micro silicon die.

Embossing forces of 5 kN, 7 kN and 9 kN were used. The loading rate was 50 N/s. Holding time was 300 seconds.

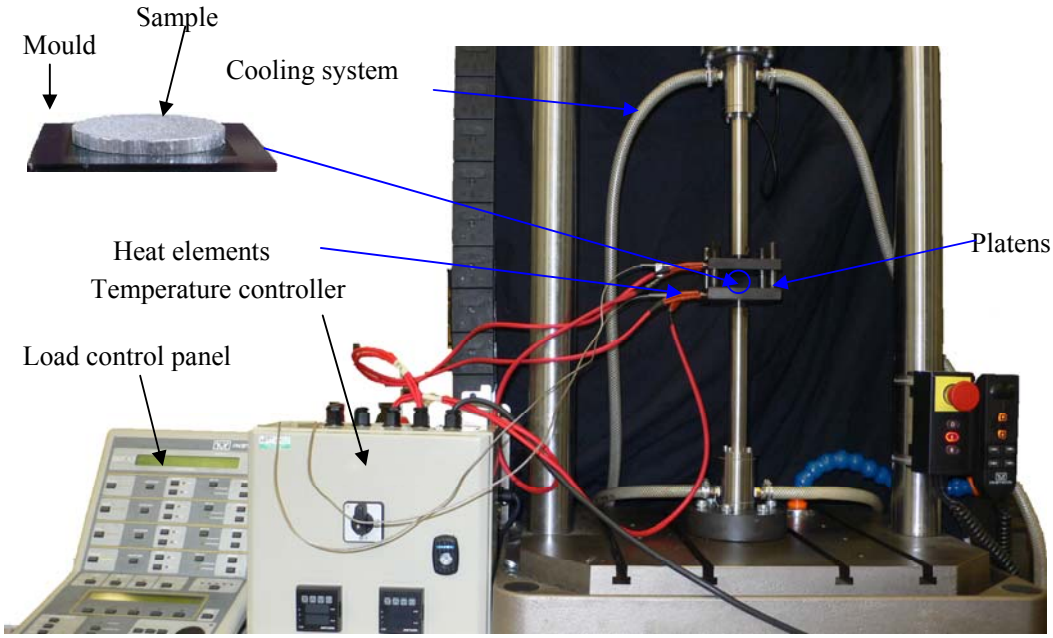

Figure 4 The embossing setup showing different components used in the experiments; the inset shows the sample and the silicon mould.

3.5. Hot embossing procedure and rigs set up

Hot embossing was carried out on the same facility used for the cold embossing. A heating system and a cooling unit were specially designed to fit the machine. Based on hardness data in Figure 5, the embossing temperature was selected as 300 ˚C. At this temperature the hardness of UFG Al-1050 dramatically decreased after annealing for half an hour but was still higher than that of fully annealed samples, which indicates the recrystallization has not completed and grains have not grown [26]. This is considered an optimum condition for embossing. A force of 3 KN was applied during embossing at 300 ˚C. The loading rate was 50 N per second. Holding time was 300 seconds.

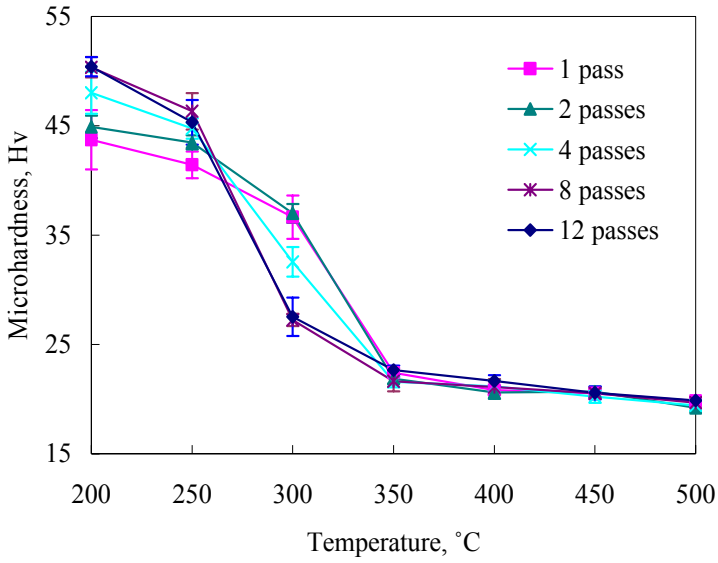

Figure5 Microhardness of UFG Al-1050 at elevated temperature.

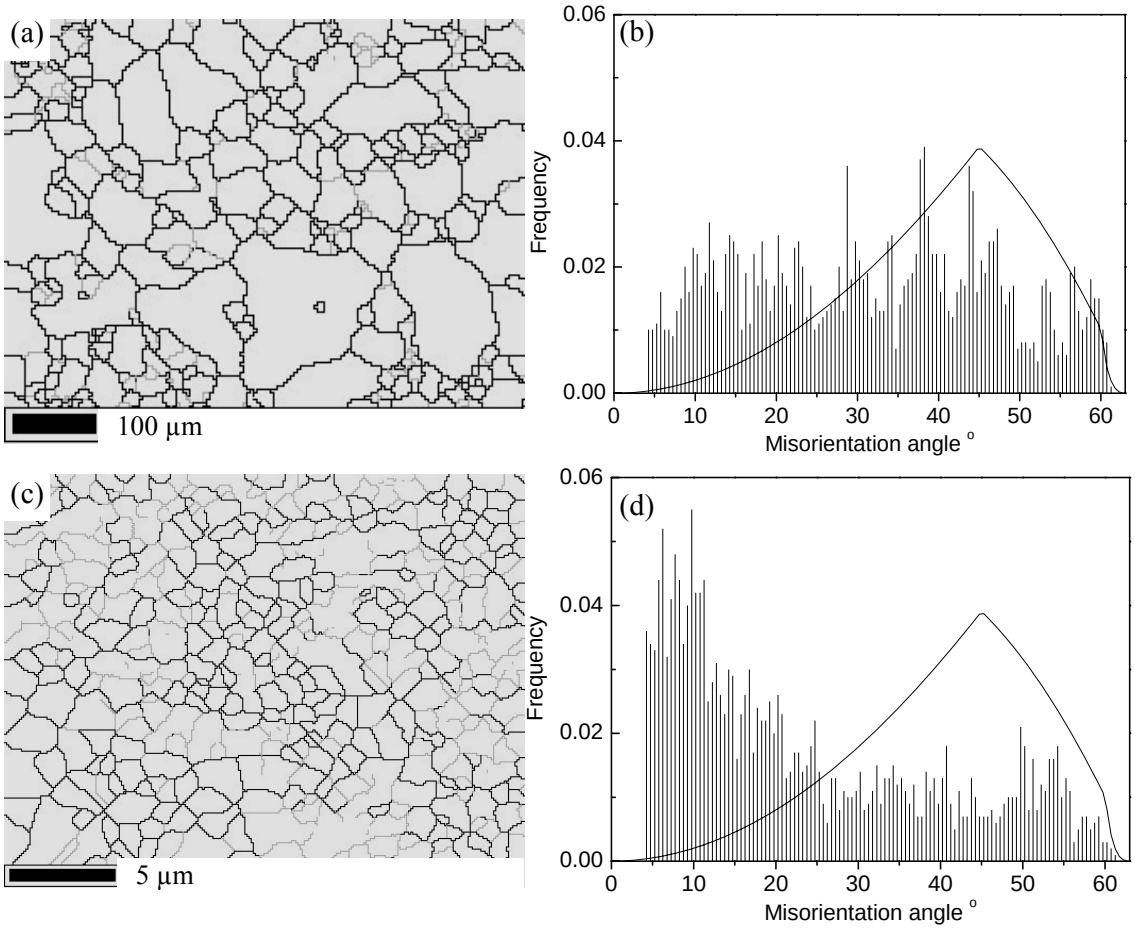

Figure 6 EBSD analysis of Al-1050 alloys. a) Orientation map and b) misorientation distribution in as-received condition; c) Orientation map and d) misorientation distribution after eight passes of ECAP. The curves in c) and d) represent the theoretical misorientation distribution of randomly oriented grains [27]

4.2. Microstructure of cold embossed foils

Figure 7 a) shows the optical microscopy (OM) image of the embossed area of the foil. The pattern on the micro silicon die was fully transferred to the foil surface. Figure 7 b) shows a high magnification SEM image of the embossed area of the foil. Some micro cracks along the longitudinal direction of the channel can be observed on the top of the grating. Some micro defects are also observed on the edge of the grating top. The defects arose because the edge of that part was broken when the micro silicon die was pressed into the foil or taken out from the foil.

Figure 8 a) and b) show the cross section of the foil mounted in resin, ground and subsequently electropolished. The electropolishing caused preferential removal of Al material near the edge of the sample, and thus the sample was not suited for detailed microscopy or EBSD. This experiment does show however that the channel depth is close to 10 µm, which is the designed embossing depth.

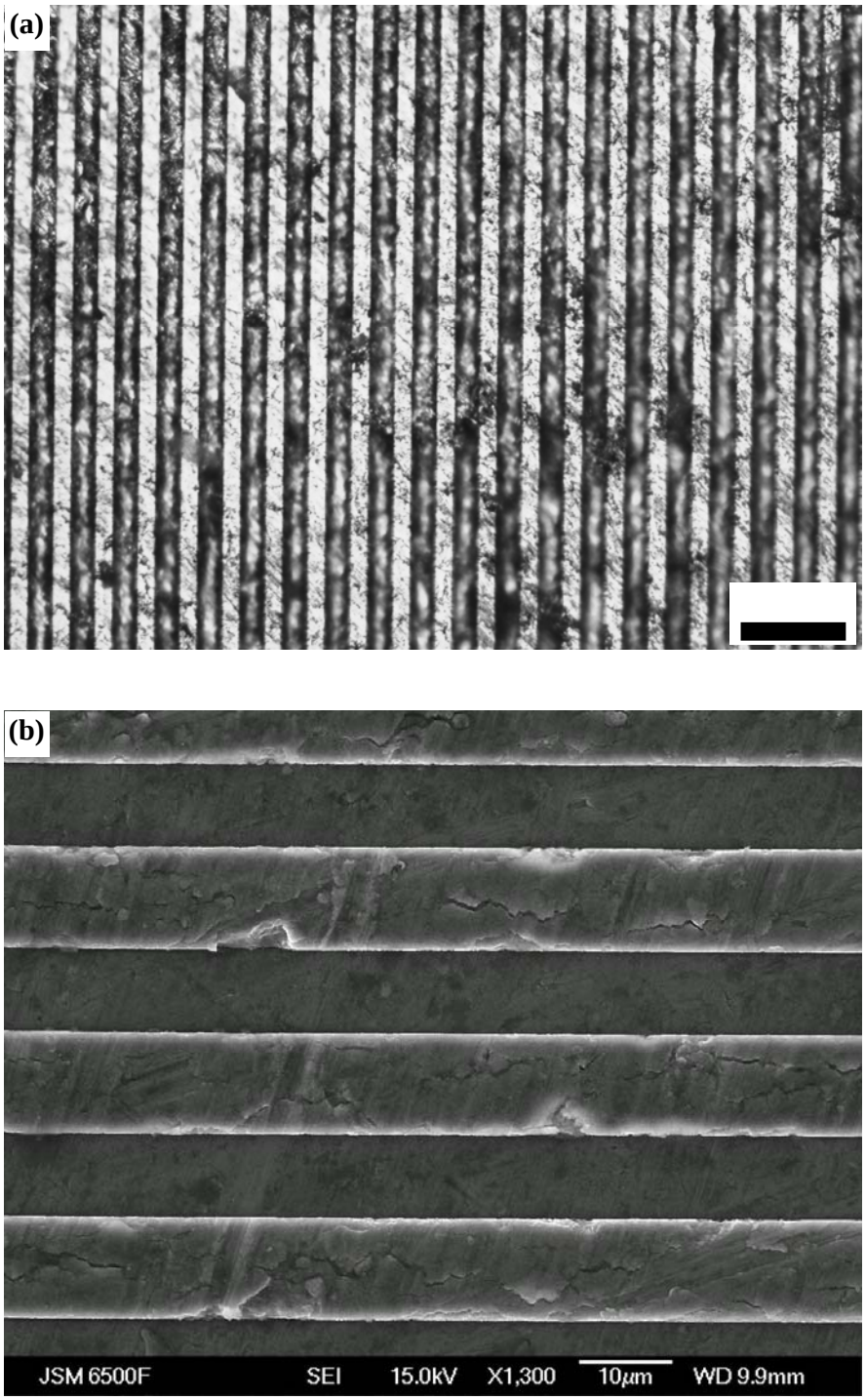

Figure 7 Embossed topography of the UFG Al-1050 foil after two passes of ECAP, the embossing force was 5kN. a) optical micrograph; b) SEM image.

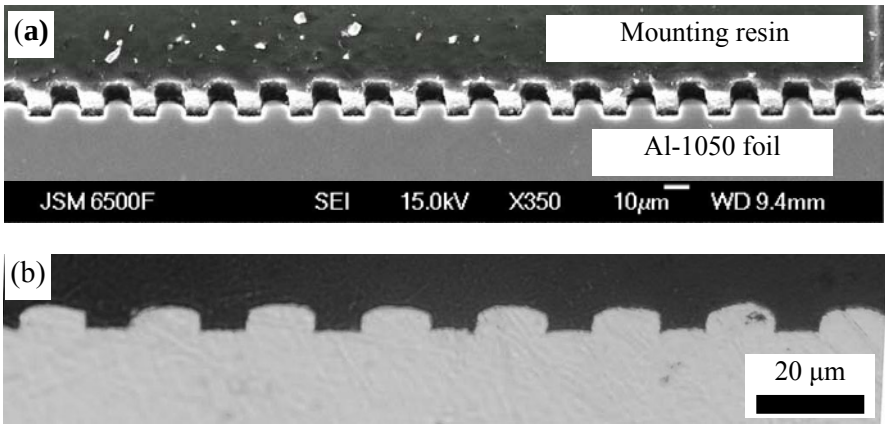

Figure 8 SEM image of the cross section of the embossed UFG Al-1050 foil, a) two passes of ECAP, SEM; b) eight passes of ECAP, OM.

4.3. Microstructure of hot embossed foils

Since a lower embossing force was applied for embossing at 300 ˚C, the failure rate of silicon mould significantly dropped, and no failures were observed in 20 pressings. Additionally, hot embossing led to a full pattern transfer from the silicon mould to the UFG aluminium foils. Figure 9 a) shows a typical SEM image of the surface of the UFG Al-1050 alloy foil embossed at 300 ˚C. The flake-like contaminants are MoS_2 used as solid lubricants. Cracks and notches, which were observed on cold embossed samples, were not observed after the hot embossing. Figure 9 b) is a FIB image of the cross-section of the UFG Al-1050 foil. The smooth part in the image centre had been milled by FIB and shows an orientation contrast. Figure 9 b) demonstrates that the depth of the channel reaches the designed value (10 μm). Moreover, the average grain size is still lower than 5 μm after hot embossing.

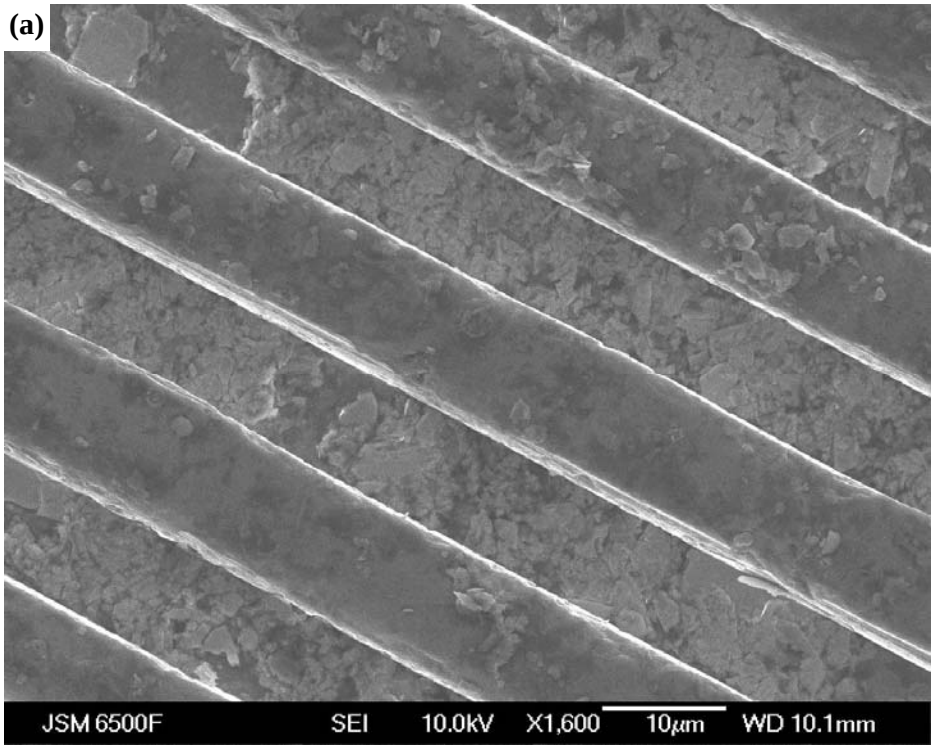

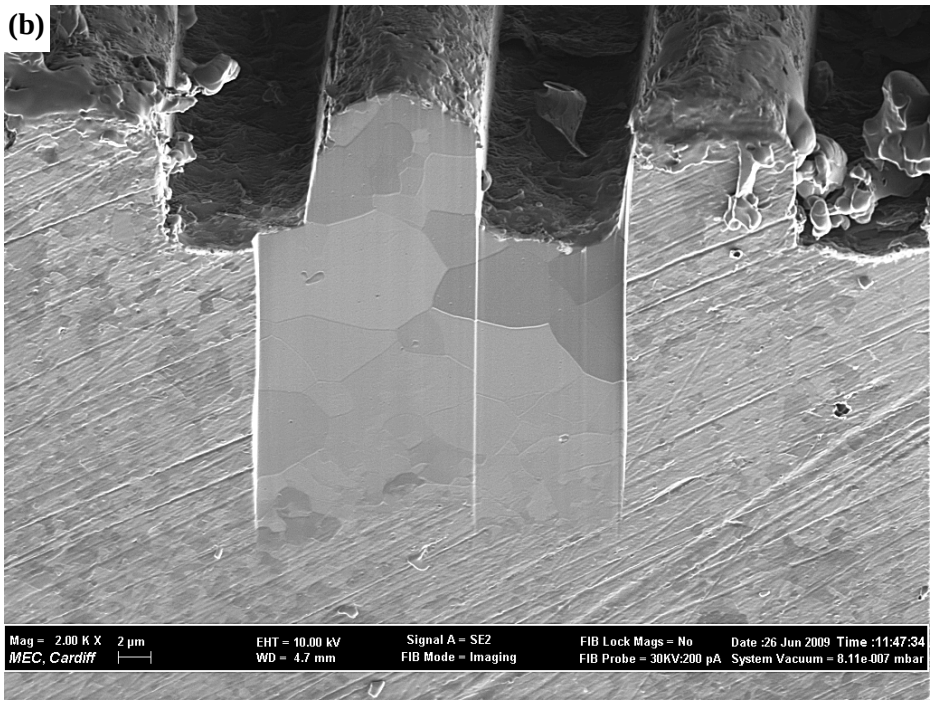

Figure 9 300 ˚C embossed UFG Al-1050 produced by eight passes of ECAP, a) Secondary electron SEM image of the top surface; b) Secondary electron FIB image of the cross-section.

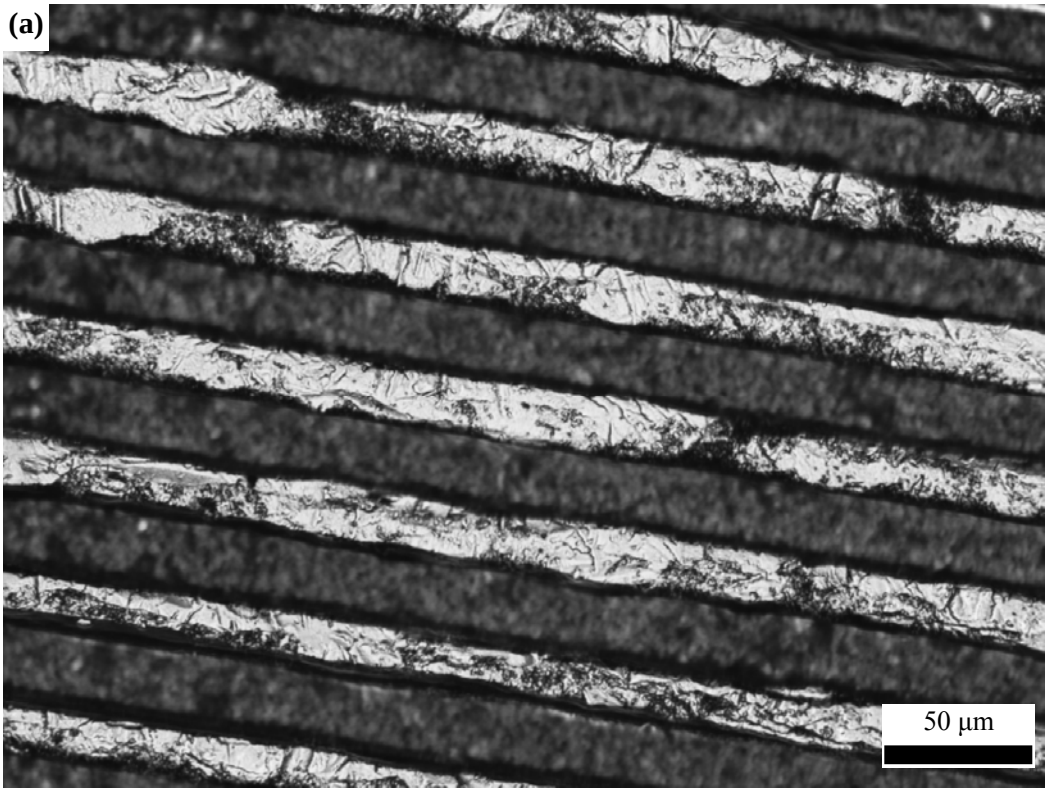

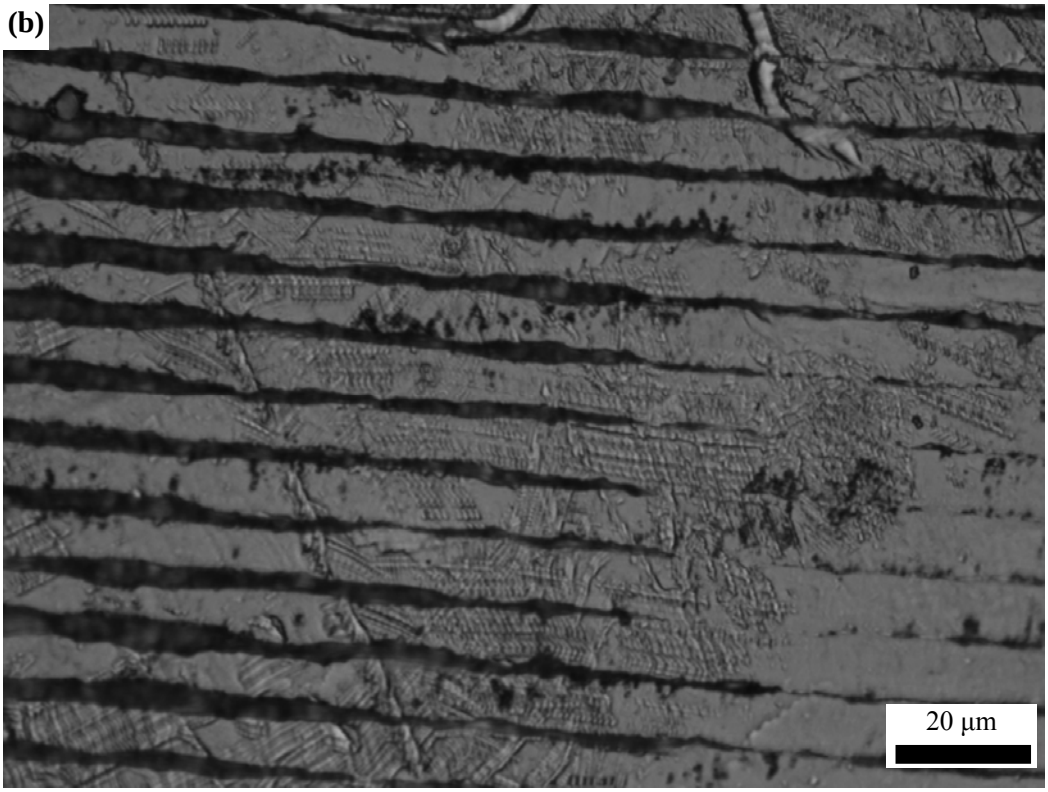

Figure 10 Optical image of 300 ˚C embossed coarse-grained Al-1050 with the channel size of a) 25 μm wide and b) 5 μm wide.

Embossing of coarse-grained Al-1050 foils at 300 ˚C has also been attempted. Figure 10 shows the topography of embossed surface of the coarse-grained Al-1050 taken by an optical microscope. The pattern on the surface was designed as parallel straight 10 μm deep channels with width of 25 μm and 5 μm. Compared to the embossed UFG foil, the channel top of the coarse-grained foil is rougher.

5. Discussion

The present experiments show good promise for application of the embossing to UFG Al foil at elevated temperature, whilst embossing at conventional grain size Al foil and embossing at room temperature were both prone to processing problems.

Under room temperature embossing only one third of the foil surface was patterned when the embossing force was set at 5 kN, rising to about 50% when the embossing force was set to 7kN or 9kN (the maximum load of the press is 10kN). Additionally, the failure rate due to the broken silicon mould dramatically increased when the embossing force was raised from 5 kN to 9 kN. The reasons for those problems are thought to be twofold. The first is that the micro silicon die is not perfectly parallel to the aluminum foil surface and does not fully contact the aluminum foil during the embossing process because of the roughness of the foil and a small residual misalignment of the platens, the micro silicon die and the foil. The micro silicon die and the foil were connected to platens, shafts, chambers and upper beam and bottom base, respectively, so that the tolerances between each part will superimpose to a certain amount of inaccurate alignment. The second reason is the inappropriate embossing force. If the embossing process is considered as a Vickers hardness test, the embossing force required can be estimated as the Vickers hardness of the embossed materials multiplied by the embossed area, i.e.:

$$F = H_V S \qquad (6)$$

where F is the embossing force, H_V is the Vickers hardness, S is embossed area. For Al-1050 after two passes of ECAP H_V is 0.44 GPa. Because of the channel structure of the die with a relation of channels and walls of 1:1 the pressed surface is half times sample area. Using Eq 6), the embossing force for Al-1050 after two passes of ECAP was calculated as 16 kN at room temperature. Due to above two factors, only a small part of aluminium foil surface was embossed when the embossing force was set as 5 kN, while more areas were embossed when the embossing force increased from 5 kN to 9 kN and the failure rate of the silicon mould went up because of the stress concentration. One potential way to resolve these problems is to ensure a perfect alignment, which will lead to full contact of the micro silicon die and the foil, but will not achieve a perfect transfer of the pattern at low force level.

The aluminium foil can be embossed by a reduced embossing force at high temperature because of the lower yield strength (and the related lower hardness) of the aluminium at high temperature. The uneven contact of the silicon mould with the aluminium foil can to some extent be evened out through creep when the embossing force is gradually applied at high temperature.

Unlike the UFG foil, the channel top of the coarse-grained foil shows many shear bands, which are thought to be caused by arrays of dislocations slipping in the same direction. The grain size of the Al-1050 in as-received condition is around 50 μm, which is two times bigger than the channel width. As a result, a channel on the silicon mould is likely to be filled by a single grain in the transverse direction, that is, dislocation movement is restricted to slipping on a preffered plane and direction. This leads to shear bands when the dislocations move out to the material surface. Figure 10 b) shows a more clear shear band, which is the OM image of the coars-grained Al-1050 foil embossed by a silicon mould of 5 μm in channel width. The pattern on the silicon mould has not been fully transferred to the coarse-grained foil and clear parallel shear bands can be seen on the surface. The angle between two crossed shear band is 60˚, which indicates the shear bands are caused by dislocation slipping on the (111)<110> slipping system.

The rounded edges of the micro channels are mainly attributed to the large grain size compared with the channel size, although spring back effect may also have a minor contribution. The micro channels made of UFG Al-1050 (1 μm grain size) are improved as compared to the caorse grained variant, but still do not posses perfect right angle edges. According to the theory in Section 2, the Al alloys with large value of K_A, e.g. Al-Mg alloys, could reach smaller grain size with the same strain. The Al-3Mg and Al-3Mg-(Sc-Zr) alloys were refined to 0.2-0.3 μm after eight passes of ECAP [27, 28]. Fabrication of micro channels using the UFG Al-Mg alloy is undergoing and will be reported in the future.

6. Summary and Conclusion

A novel process for the fabrication of a microelectromechanical systems (MEMS) metallic component with features smaller than 10 μm and high thermal conductivity was investigated. In the first stage of processing, an ultra fine grained (UFG) Al-1050 was produced by equal channel angular pressing (ECAP). Conclusions are drawn as follows:

1) Cold embossing of the UFG Al-1050 leads to a high failure rate of micro silicon mould and an incomplete pattern transaction from the silicon mould to the foil.
2) Hot embossing of the coarse-grained Al-1050 produces channels that are not smooth, but embossing of the UFG Al-1050 at 300 ˚C produces smooth channels. The pattern on the micro silicon mould is fully transferred to the foil surface.
3) Hot embossing at 300 ˚C allows a reduced embossing force to be used.
4) Embossing of ECAP processed UFG aluminium alloys has shown a good potential for application in microdevice fabrication.

Acknowledgement:

This work was funded by Engineering Physics Science Research Council under Grant No. EP/D00313X/1. The FIB work was funded under grant No. EP/F056745/1. Author XGQ thanks ORSAS and School of Engineering Sciences of University of Southampton for additional studentship funding. Prof. S.M. Spearing and Dr. Liudi Jiang (University of

Southampton) are gratefully acknowledged for valuable discussion. Dr. Georgi Lalev (University of Cardiff) is gratefully acknowledged for FIB work.

.

References:

[1] Tuckerman D B and Pease R F 1981 *IEEE Electron Device Lett.* **2** 126-29
[2] Jiang P X, Fan M H, Si G S and Ren Z P 2001 *Int. J. Heat Mass Transfer* **44** 1039-51
[3] Chang C, Wang Y F, Kanamori Y, Shih J J, Kawai Y, Lee C K, Wu K C and Esashi M 2005 *J. Micromech. Microeng.* **15** 580–85
[4] Hardt D, Ganesan B, Dirckx M, Shoji G, Thaker K and Qi W 2005 *Innovation in Manufacturing Systems and Technology* IMST(2005)01
[5] Friedrich C R and Kang S D 1994 *Preci. Eng.* **16** 56-59
[6] Schubert K, Brandner J, Fichtner M, Linder G, Schygulla U and Wenka A 2001 *Microscale Thermophys. Eng.* **5** 17–39
[7]Brandner J J, Anurjew E, Bohn L, Hansjosten E, Henning T, Schygulla U, Wenka A and Schubert K 2006 *Exp. Therm Fluid Sci.* **30** 801-09
[8] Bier W, Keller W, Linder G, Seidel D and Schubert K 1990 Winter Annual Meeting of the American Society of Mechanical Engineers (Dallas, TX, USA 25-30 November 1990) (American Society of Mechanical Engineers, Dynamic Systems and Control Division vol 19) pp189-97
[9] Otto T, Schubert A, Böhm J and Gessner T 2000 Micromachining Technology for Micro-Optics (Santa Clara, USA, 20 September 2000) (Proc. SPIE – Int. Society for Optical Engineering vol 4179) ed. Lee S H and Johnson E G (Bellingham, WA: Society of Photo-Optical Instrumentation Engineers) pp 96–106
[10] Jiang J, Mei F, Meng W J, Sinclair G B and Park S, 2008 *Microsyst. Technol.* **14** 815–19
[11] Böhm J, Schubert A, Otto T and Burkhardt T 2001 *Microsystem Tech.* **7** 191-95
[12] Valiev R Z, Estrin Y, Horita Z, Langdon T G, Zehetbauer M J and Zhu Y T 2006 *JOM* **58** 33-39
[13] Starink M J, Qiao X G, Zhang J, Gao N, 2009 *Acta Mater.* **57** 5796-11
[14] Valiev R Z, Islamgaliev R K and Alexandrov I V, 2000 *Prog. Mater. Sci.* **45** 103-89
[15] Valiev R Z, Langdon T G 2006 *Prog.Mater. Sci.* **51** 881–981
[16] Gao N, Starink M J, Furukawa M, Horita Z, Xu C, Langdon T G 2005 *Mater. Sci. Eng.* A **410-411** 303-07
[17] Baretzky B *et al* 2005 *Rev. Adv. Mater. Sci.* **9** 45-108.
[18] Justinger H and Hirt G 2009 *J. Mater. Proc. Tech.* **209** 2111-21
[19] Saotome Y, Zhang T and Inoue A 1999 Proc. 1998 MRS Fall Meeting – Symp. MM on Bulk Metallic Glasses (*Boston MA, USA, 1-3 December 1998*) in: Mat. Res. Soc. Symposium Proc vol 554 pp 385–390
[20] Segal V M, Hartwig K T and Goforth R E 1997 *Mater. Sci. Eng.* A **224** 107-15
[21] Iwahashi Y, Wang J T, Horita Z, Nemoto M and Langdon T G 1996 *Scripta Mater.* **35** 143-46
[22] Prangnell P B, Harris C and Roberts S M, *Scripta Mater.* **37** 983-89
[23] Wu Y and Baker I 1997 *Scripta Mater.* **37** 437-42
[24] Langdon T G, Furukawa M, Nemoto M and Horita Z 2000 *JOM* **52** 30-33
[25] Nakashima K, Horita Z, Nemoto M and Langdon T G 2000 *Mater. Sci. Eng.* A **281** 82-87
[26] Qiao X G, Starink M J and Gao N 2009 *Mater. Sci. Eng.* A **513–514** 52–58
[27] Hasegawa H, Komura S, Utsunomiya A, Horita Z, Furukawa M, Nemoto M and Langdon T G 1999 *Mater. Sci. Eng* .A **265** 188-196
[28] Lee S, Utsunomiya A, Akamatsu H, Neishi K, Furukawa M, Horita Z, Langdon TG 2002 *Acta Mater.***50** 553-64